Magnetic activity in stars and its effects on their astrospheres

Scientific report

This report is a summary of our most important scientific results achieved in the framework of the NKFIH research contract K131508. Most of the following results have already been published in high-impact journals.

Preamble

It is generally accepted that the Sun and similar (low mass) main sequence stars are able to provide a relatively stable cosmic environment for billions of years, thereby providing favorable conditions for life to grow up on the surface of rocky planets orbiting at a suitable distance. On the way to the formation of terrestrial life, we attribute an important role to solar activity from the point of view of biochemical evolution. At the same time, it is also known that magnetic activity itself can even be one of the main threats to habitability. That is why we focused our research on the investigation of the origin of solar and stellar magnetic activity, as well as the effect of magnetism on the cosmic environment.

The mechanism behind solar and stellar activity is the magnetic dynamo, so we took its observable components as the subject of our investigation. Observing solar activity allows a much deeper insight into the manifestations of the dynamo than we can currently hope for in the case of stars. Understanding solar activity therefore helps to bring closer the magnetic activity processes taking place in the convective layers of distant stars. In light of all this, we have compared solar and stellar magnetic activity in order to understand how unique or regular our Sun is in the pool of active stars, while the issue of habitability was also part of our research. We examined how the structure of the magnetic fields of the stellar surfaces changes in the case of different types of active stars. We investigated how tidal interactions in binary and multiple star systems affect stellar activity. One of our investigations even led to the accidental discovery of a faint eclipsing binary subsystem in an interesting 2+2 hierarchical quadruple star system called V815 Her. Finally, we note that in our latest study (currently in the second round of review in Nature Communications) we processed a unique 16-year spectroscopic data series of XX Tri, the "most spotted" star in the sky, which points to the chaotic operation of the dynamo in the star. Our new scientific results achieved during the project are summarized as follows.

1 The solar paradigm of stellar magnetism—a closer look

Solar observations played an important role in our research program from the point of view of the analogy of solar and stellar activity. Below is a summary of some of our most interesting solar activity studies.

We used photospheric magnetic field maps from the past four solar cycles and found that the fractional contribution of active regions to the solar wind varied between 30% to 80% at any one time during solar maximum and it was negligible at solar minimum, showing a strong correlation with sunspot number.

We examined the driving mechanism of the very strong upflows, known as blue-wing asymmetries, in the solar atmosphere during the eruption of a flux rope and found that the mechanism driving the strongest upflows was the same as the one driving the persistent (weaker) upflows observed in all solar active regions. By studying hot flux ropes in the solar corona we have inferred that the orbital motions of photospheric magnetic flux fragments about each other bring magnetic flux tubes together in the corona, enabling component reconnection that forms a magnetic flux rope above a flaring arcade. This represents a novel trigger mechanism for solar coronal mass ejections (hereafter CME) and should be considered when predicting solar magnetic activity.

NOAA Active Region (AR) 12967 was tracked simultaneously by Solar Orbiter at 0.35 AU and Hinode/EIS at Earth. During the three day-long observing period, strong blueshifted plasma upflows were observed along a thin, dark corridor of open magnetic field originating at the AR's leading polarity and continuing toward the southern extension of the northern polar coronal hole. A potential field source surface model shows large lateral expansion of the open magnetic field along the corridor. Squashing factor Q-maps of the large-scale topology further confirm super-radial expansion in support of the S-web theory for the slow wind. The thin corridor of upflows is identified as the source region of a slow solar wind stream. When the connectivity changes from the corridor to the eastern side of the AR, the in situ plasma parameters of the slow solar wind indicate a distinctly different source region. These observations provide strong evidence that the narrow open-field corridors, forming part of the S-web, produce some extreme properties in their associated solar wind streams.

We participate in the ongoing recalibration of the Wolf sunspot number (SN) and group-sunspot number (GN) following the release of version 2.0 of SN in 2015. The current report constitutes both an update of the efforts reported in the 2016 Topical Issue of Solar Physics and a summary of work by the International Space Science Institute (ISSI) International Team formed in 2017 to develop optimal SN and GN reconstruction methods while continuing to expand the historical sunspot-number database. New versions of the underlying databases for SN and GN will shortly become available for years through 2022 and we anticipate the release of the next versions of these two time series in 2024.

2 FIP and inverse-FIP effect in the solar and stellar coronae

Placing solar and stellar activity on a common platform was most beneficial in the following topic. In the solar corona elements of low first ionisation potential (FIP) are enhanced by a factor of 3-4 compared to their photospheric abundances ('FIP-effect'). On the other hand, recent observations have shown that, 'inverse-FIP' regions (or 'I-FIP' for short), i.e. enhanced abundances of high-FIP elements (or depleted low-FIP elements) could also be found in the photosphere near sunspots in flare spectra. To date, there is only one model, which is able to explain FIP and I-FIP coronal abundances in a consistent way, which invokes the ponderomotive force exerted by Alfvén waves giving rise to ion-neutral separation in stellar chromospheres. The direction of the ponderomotive force (i.e., Alfvén waves of either coronal or sub-photospheric origin) defines whether low-FIP elements become enhanced (FIP) or depleted (I-FIP) in the corona. We have produced many interesting results in this topic, and in our extensive work, which investigated such effects in 59 stars, we provided the most comprehensive analysis of the topic so far from an observational point of view.

We observed four localized patches of I-FIP effect solar plasma in active region AR 12673. We conclude that plasma with I-FIP effect composition was created by the refraction of waves coming from below the chromosphere. We propose that the waves generating the I-FIP effect plasma in solar active regions are generated by subphotospheric reconnection of coalescing flux systems.

We analyzed the evolution of the coronal plasma composition in a solar active region as well as the coronal elemental abundances during a small solar flare. We observed a strong increase in coronal abundance of Ca XIV 193.84 Å, an emission line with low first ionization potential (FIP <10 eV), as quantified by the ratio Ca/Ar during the flare. This is in contrast to the unchanged abundance ratio observed using Si X 258.38 Å/S X 264.23 Å. We proposed two different mechanisms to explain the different composition results. We investigated the spatial distribution of highly varying plasma composition around one of the largest sunspots. Our results indicate a connection between sunspot chromospheric activity and observable changes in coronal plasma composition.

FIP-effect is often observed in the slow-speed (<500 km s^{-1}) solar wind and in solar-like stellar coronae, while inverse-FIP composition appears to dominate cool, fully convective, flaring M-dwarf stars. We observed several inverse events in the slow solar wind using particle-counting techniques. These very rare events all occur during periods of high solar activity that mimic conditions more widespread on M dwarfs. The results imply that M-dwarf winds are dominated by plasma depleted in easily ionized elements and lend credence to previous spectroscopic measurements.

We present a survey of coronal elemental composition as expressed in the first ionization potential (FIP) bias in 28 solar active regions (ARs) of different ages and magnetic

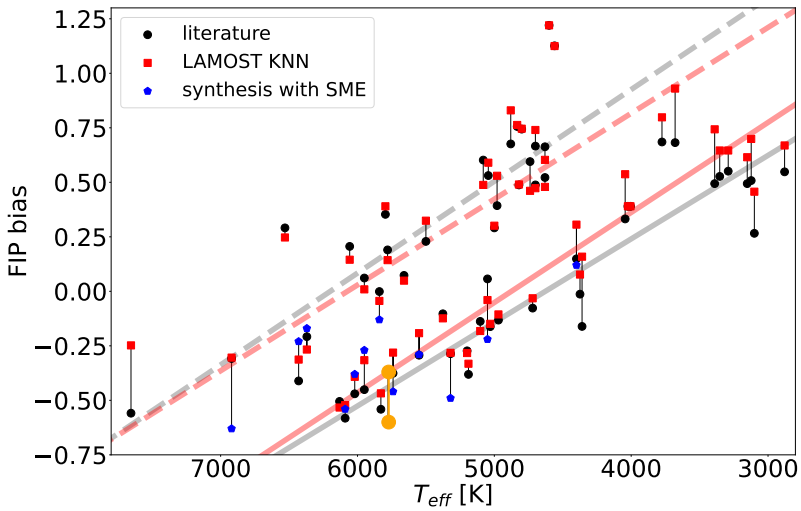

Figure 1: $T_{\rm eff}$−FIP-bias diagram with recalculated FIP-bias values. For the Sun, orange points mark its activity minimum and maximum. Solid and dashed lines show two component linear fits with a RANSAC regressor, with grey and red corresponding to literature and the KNN FIP bias, respectively (Seli et al. 2022).

flux content, which are at different stages in their evolution. Our findings indicate that, while some general trends can be observed, the processes influencing the composition of an AR are complex and specific to its evolution, magnetic configuration, or environment. The spread of FIP bias values in ARs shows a broad match with that previously observed in situ in the slow solar wind.

In a more extended study we compiled FIP bias and other parameters for 59 stars for which coronal composition is available, now including evolved stars. We find three clusters in the FIP bias determinant parameter space: evolved stars form a separate group. The two other groups of active main sequence stars represent a transition in dynamo type in connection with the FIP bias. We find that the $T_{\rm eff}$−FIP-bias diagram is not a simple relation as thought before, but it now has two branches separated by $\sim$0.5 in FIP bias; see **Fig. 1**. The new (upper) branch consists of mostly evolved stars and additionally stars with high rotational velocity. The low-mass, flaring M dwarfs form a small blob in the continuation of the lower branch of the relation. These new results challenge the FIP-bias paradigm.

Solar magnetic flux ropes are bundles of twisted magnetic field enveloping a central axis. They harbor free magnetic energy and can be progenitors of CMEs. We analyze the coronal plasma composition in AR 10977 and its evolution as a sigmoid (flux rope) forms and erupts as a CME. Plasma with photospheric composition was observed in coronal loops close to the main polarity inversion line during episodes of significant flux cancellation, suggestive of the injection of photospheric plasma into these loops driven by photospheric flux cancellation. Concurrently, the increasingly sheared core field contained plasma with coronal composition. As flux cancellation decreased and a sigmoid/flux rope formed, the plasma evolved to an intermediate composition in between photospheric and typical AR

coronal compositions. Finally, the flux rope contained predominantly photospheric plasma during and after a failed eruption preceding the CME. Hence, plasma composition observations of AR 10977 strongly support models of flux rope formation by photospheric flux cancellation forcing magnetic reconnection first at the photospheric level then at the coronal level.

We studied the plasma composition in a solar active region following an episode of significant new flux emergence into the preexisting magnetic environment of the active region. We observed slightly higher FIP bias values with the Ca/Ar diagnostic than Si/S in the newly emerging loops, and this pattern is much stronger in the preexisting loops (those that had been formed before the flux emergence). This result can be interpreted in the context of the ponderomotive force model, which proposes that the plasma fractionation is generally driven by Alfvén waves. Model simulations predict this difference between diagnostics using simple assumptions about the wave properties, particularly that the fractionation is driven by resonant/nonresonant waves in the emerging/preexisting loops. We propose that this results in the different fractionation patterns observed in these two sets of loops.

3 Stellar activity—a broader view

3.1 Flares, superflares and stellar CMEs

We analyzed the 30 min cadence TESS light curves of 248 stars, searching for flares and rotational modulation caused by starspots. The composite flare frequency distribution of the 94 identified flares showed a power-law index similar to that of the M-type red dwarf TRAPPIST-1.

We analyzed the flaring activity of KIC 2852961, a late-type giant star, in order to understand how its flare statistics are related to those of other stars with flares and superflares. We concluded that there might be a scaling effect behind the generation of flares and superflares in the sense that the higher the magnetic activity, the higher the overall magnetic energy released by flares and/or superflares.

We carried out a comprehensive study of flaring giant stars in the Kepler field. We found no strong correlation between the stellar properties and the flaring characteristics. The wide scale of the flaring specialities are hardly related to the giant nature, if at all, supporting that there is a common background physics in flaring stars.

We studied the occurence of CMEs of solar-like stars by using spectroscopic data from the ESO phase 3 and Polarbase archives. We found no signatures of CMEs and only few flares. The non-detection of CMEs was compared with empirically modelled CME rates. We concluded that the on-source times were mostly too short to detect stellar CMEs and the non-detections are related to observational biases in conjunction with a low level of activity of the investigated dF-dK stars.

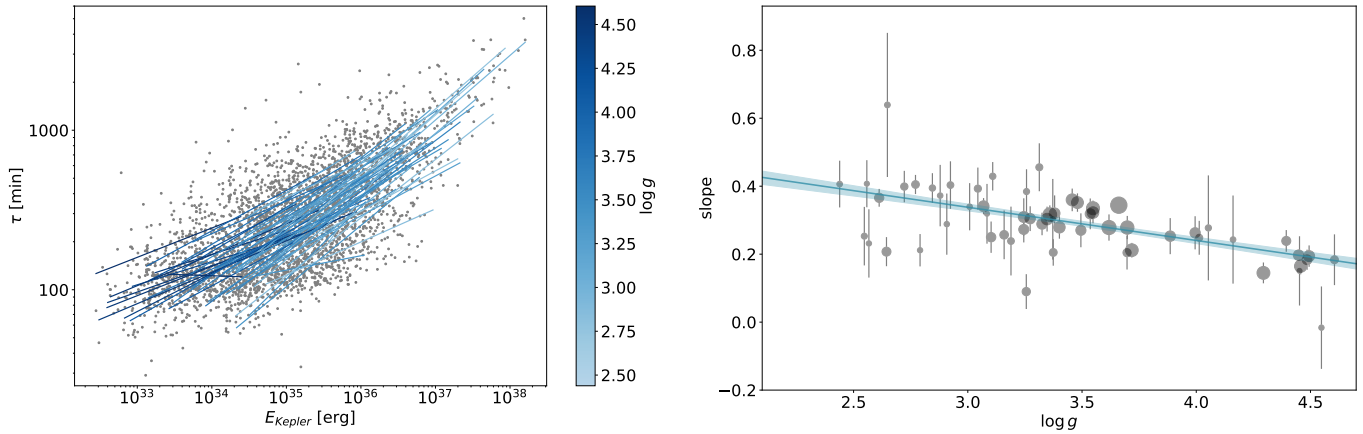

Figure 2: Flare duration vs. flare energy for *Kepler* giants (Oláh et al. 2022). *Left:* τ flare duration values for flares in the *Kepler* 30-min sample as a function of flare energy on a log-log scale with linear fits to the values of individual stars. *Right:* slopes of the fitted lines from the left panel as a function of $\log g$. Error bars show the uncertainties of the slopes, the point sizes represent the number of flares observed on each star. The blue line shows a linear fit.

Although late-type dwarfs and giant stars are substantially different, their flares are thought to originate in similar physical processes and differ only by a scale factor in the energy levels. We studied the validity of this approach. We searched for characteristics of flares on active giants, which might be statistically different from those on main-sequence stars. We used nearly 4000 flares of 61 giants and 20 stars of other types that were observed with Kepler satellite. Strong correlations were found between the flare duration and the surface gravity, luminosity, and radii of the stars. We conclude that the generalized linear scaling for the logarithmic relation of flare energy and duration with a universal theoretical slope of $\approx$1/3 should slightly be modified by introducing a dependence on surface gravity (see **Fig. 2**).

3.2 Stellar dynamos in close binaries

Close binaries with magnetically active components are astrophysical laboratories for studying the effects of binarity on activity. Of particular interest are binary and multiple star systems that contain a solar-type active component with an internal structure similar to the Sun, allowing us to study how the dynamo of a solar-type star would work under different conditions.

We studied the eclipsing binary system V471 Tau, a red dwarf-white dwarf close binary, and showed that the magnetic activity of the red dwarf component is strongly influenced by the close hot companion. The detected weak differential rotation of the red dwarf is very likely the result of tidal confinement by the companion. We showed that the periodic appearance of the inter-binary Hα emission from the vicinity of the inner Lagrangian point is correlated with the activity cycle.

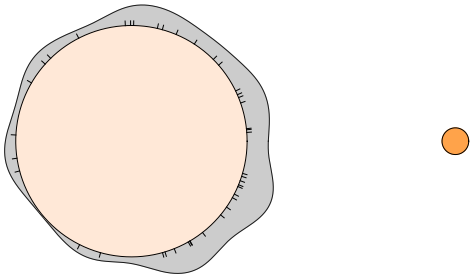

Figure 3: The flare occurrence distribution in the frame of the orbital phase on the active component in the close binary system EI Eri (Kriskovics et al. 2023). The distribution function (in grey) suggests that the gravity of the secondary star affects the appearance of the flares. The size and distance of the stars are shown to scale.

We used our photometric time series of more than 40 yr to analyze the long-term behavior of the single-lined spectroscopic binary EI Eri. We investigated flare activity using photometric data obtained with the Transiting Exoplanet Survey Satellite (TESS) and found that flares occur more frequently in phases facing the secondary component (see **Fig. 3**). We used uninterrupted MUlti-SIte Continuous Spectroscopy (MUSICOS) campaign data of EI Eri to reconstruct successive surface-temperature maps of the star in order to study the changes of starspots on a very short timescale. The time-resolved spotted surface of EI Eri from Doppler imaging enabled us to follow the evolution of the different surface features. Cross-correlating the consecutive Doppler maps revealed a surface shear of $\Delta\Omega/\Omega_{\rm eq}$=0.036$\pm$0.007.

We were conducting a comprehensive investigation of V815 Her, formerly known as a triple system, to understand the origin of the activity of its G-type primary component and what influences it in the short and long term. From TESS photometry we found evidence that the V815 Her B component previously apostrophized as a 'third body' is actually an eclipsing close binary subsystem of two M dwarfs with an orbital period of 0.5 d. From our spectroscopic data covering 200 days we created 19 time-series Doppler images of the G-type primary V815 Her Aa. Spot activity on the primary was found to be vivid, spots were redistributed on a time scale of a few weeks. Fast starspot decay suggests that convective-turbulent erosion plays a more significant role in such a rapidly rotating star. The weak surface differential rotation found for the G-star is presumably confined by tidal forces of the close (most likely late M-type) companion V815 Her Ab. The slowly increasing photometric cycle of about 6.5 years on average is interpreted as a spot cycle of the G-star, which is probably modulated by the eccentric wide orbit.

We presented a 16-year long time series of Doppler images for XX Tri, the "most spotted" star in the sky. Creating this unique times series was only possible thanks to the continuous operation of the STELLA robotic telescope on Tenerife and its high-resolution echelle spectrograph SES. The robot has observed the star on every available clear night since July 2006, acquiring a total of over 2000 high-resolution, high signal-to-noise-ratio (S/N) spectra that are used to create 99 independent Doppler images. We combine these

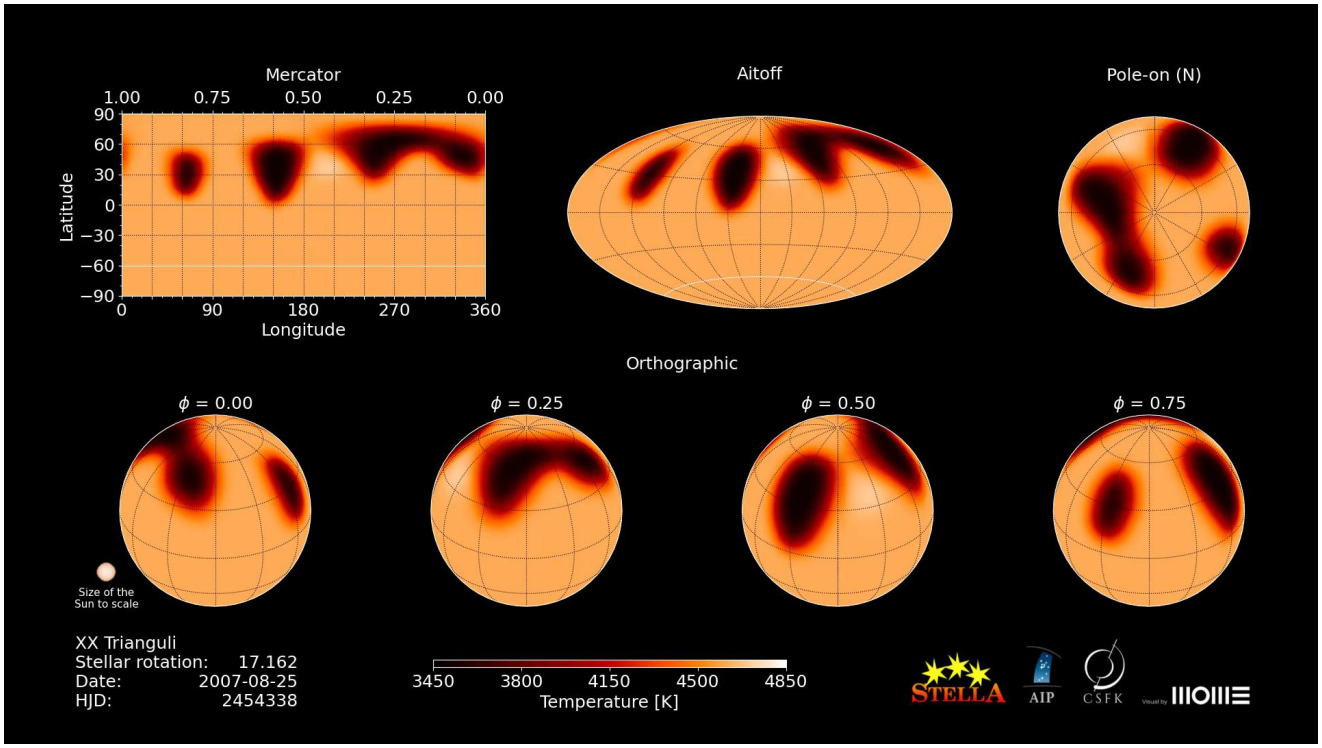

Figure 4: The GUI layout of the main movie in Strassmeier, Kővári, Weber & Granzer (2024). The spotted surface of XX Tri is presented in four different projection styles. In the top row, from left to right, equidistant Mercator projection, true area Aitoff projection, and a pole-on view. The bottom row is a phase-resolved orthographic projection for four rotational phases. Time is counted in stellar rotations, in civil date, and in HJD. The real-time coverage is 237 stellar rotations from August 2006 to February 2022 (∼16 years) or 5670 days. Surface color is always coded in terms of temperature as defined in the color bar.

images into a movie visualizing XX Tri's surface spot evolution for the past 16 years, see **Fig. 4**. Based on our unique long-term data, we infer a mostly chaotic, probably non-periodic dynamo in the case of XX Tri.

4 Circumstellar material around young low mass stars

Very young, low mass pre-main-sequence stars are astrophysical laboratories to study the evolution of protoplanetary material and its interaction with the central star. The activity of such stars, often associated with magnetic star-disc interactions, significantly affects the circumstellar environment. The accretion disk surrounding the star can be considered the cradle of emerging planets. However, to interpret the paralell processes correctly, we need to disentangle the signals related to disk–stellar interactions from those related to stellar magnetic activity (starspots, flares, etc.). The steps we have taken in this direction are summarized below.

Among such targets, we highlight DE Boo here, which is a unique system, with an edge-on view through the debris disk around the star. The disk, which is analogous to the Kuiper belt in the Solar System, was reported to extend from 74 to 84 AU from the central star. The high photometric precision of the Characterising Exoplanet Satellite (CHEOPS)

provided an exceptional opportunity to observe small variations in the light curve due to transiting material in the disk. We found nonperiodic transient features in the residual light curves with a transit duration of 0.3–0.8 days. We calculated the maximum distance of the material responsible for these variations to be 2.47 AU from the central star, much closer than most of the mass of the debris disk. Moreover, it was the first time that flaring events were observed in this system. We interpreted the transient features as the result of scattering in an inner debris disk around DE Boo. The processes responsible for these variations were investigated in the context of interactions between planetesimals in the system.

New sets of young M dwarfs with complex, sharp-peaked, and strictly periodic photometric modulations have recently been discovered with Kepler/K2 (scallop shells) and TESS (complex rotators). All are part of star-forming associations, are distinct from other variable stars, and likely belong to a unified class. Suggested hypotheses include starspots, accreting dust disks, corotating clouds of material, magnetically constrained material, spots and misaligned disks, and pulsations. From our investigation we suggest a unified hypothesis, a superposition of large-amplitude spot modulations and sharp transits of corotating gas clouds.

5 Stellar environment and habitability

After examining the components of the evolution of circumstellar environment in the results listed so far, such as the evolution of the accreted material around very young stars and stellar magnetic activity, we have arrived at the subject of exoplanets and the related question of habitability.

TRAPPIST-1, an ultracool red dwarf is surrounded by seven planets configured in a resonant chain. We run numerical simulations using fictitious forces of trapping the fully grown planets in resonances as they migrated in the gas disc, followed by numerical simulations detailing their tidal evolution. We show that the current eccentricities and spacing of planets “d” to “h” are natural outcomes of coupled tidal evolution wherein the planets simultaneously damp their eccentricities and separate due to their resonant interaction.

We modelled the interiors of 28 habitable zone rocky exoplanets, assuming four different layers - an iron core, a rock mantle, a high-pressure ice layer, and a surface ice/water layer. We determined a range of possible water mass fractions for each planet consistent with the modelled planetary structures. We calculated the tidal heating experienced by these exoplanets through gravitational interactions with their host stars. Assuming radioactive elemental abundances observed in Solar System meteorites, we also calculated the radiogenic heat flux inside the planets. We estimated the probability of the presence of a thick ocean layer in these planets, taking into account the effect of both tidal and radiogenic heating. Our results showed that Proxima Centauri “b”, Ross 128 “b”, Teegarden’s “b” and “c”, GJ 1061 “c” and “d”, and TRAPPIST-1 “e” may have an extended liquid

water reservoir. Furthermore, extremely high H_2O-content of the exoplanets Kepler-62 "f", Kepler-1652 "b", Kepler-452 "b", and Kepler-442 "b" suggests that these planets may maintain a water vapour atmosphere and may in fact be examples of larger ocean worlds.

We investigated the habitability of hypothetical moons orbiting known exoplanets. We calculated the incident stellar radiation and the tidal heating flux arising in the moons as the two main contributors to the energy budget. We used the runaway greenhouse and the maximum greenhouse flux limits as a definition of habitability. We provided a target list for observations of known exoplanets of which the top 10 planets have more than 50% chance for hosting habitable moons on stable orbits. In this context, we studied the long-term stability of hypothetical exomoon orbits around known exoplanets. We found that tidal instability causes moons to escape or being tidally disrupted around close-in planets having <10 days orbital periods.

6 Publication activity in numbers

Altogether 42 publications were listed in the closing report; 39 were published as refereed papers, mostly in high-impact journals (among them, the latest one is under the second round of revision in Nature Communications). Our four-year publication activity resulted in a cumulative impact factor of 221.63.